

Supporting Information

L-Proline-methyl ester derivatives-modulated synthesis of gold nanoclusters with promoted peroxidase-mimic activity for monitoring of ofloxacin

Xinya Zhang^{1,2}, Juan Qiao^{1,3}, Wei Liu^{2*}, Li Qi^{1,3*}

¹ Beijing National Laboratory for Molecular Sciences; Key Laboratory of Analytical Chemistry for Living Biosystems, Institute of Chemistry, Chinese Academy of Sciences, Beijing 100190, P.R. China

² School of Pharmacy, Xinxiang Medical University, Xinxiang 453003, P. R. China

³ School of Chemical Sciences, University of Chinese Academy of Sciences, Beijing 100049, P. R. China

* **Correspondence authors:** Wei Liu, Li Qi

liuwei@xxmu.edu.cn

qili@iccas.ac.cn

Experimental procedures

Instruments

The ultraviolet-visible (UV-vis) absorption spectra were recorded using a TU-1900 UV-vis double-beam spectrometer (Purkinje General, China). A 1.0 mL capacity cuvette with a 1.0 cm path length was used for measuring the UV-vis absorbance.

The fluorescence measurements were performed using an F-4600 fluorescence spectrophotometer (Hitachi, Japan).

Fourier transform infrared (FT-IR) spectra were recorded by an FT-IR spectrophotometer (TENSOR-27, Germany).

The zeta potential measurements were carried out with a Zetasizer laser particle analyser (Zetasizer Nano ZS ZEN3600, British).

X-ray photoelectron spectroscopy (XPS) measurements were performed by an ESCALab220i-XL spectrometer (VG Scientific, U.K.).

Transmission electron microscopy (TEM) images were obtained using a transmission electron microscope (JEM-2010, Japan electron optics laboratory, Japan) at a voltage of 200 kV.

Electrospray ionization mass (ESI-mass) spectrometry (Bruker Q-TOF II, Germany) was used to analyze the chemical constituents of AuNCs solutions.

Electron paramagnetic resonance (EPR) signals were measured by a Bruker ESP 300E spectrometer (Bruker, Rheinstetten, Germany) with a microwave bridge (receiver gain, 1×10^5 ; modulation amplitude, 2 Gauss; microwave power, 10 mW; modulation frequency, 100 kHz). A sample containing 0.1 M DMPO was transferred to a quartz capillary tube and placed in the EPR cavity. Under the UV-irradiation at 355 nm, EPR signals were detected using DMPO as the spin trap.

Preparation of Pro@AuNCs, PAM@AuNCs and HYP@AuNCs

All glassware was washed with aqua regia (1:3 HNO₃: HCl) and rinsed with ethanol and double distilled water. In a typical experiment, HAuCl₄ solution (6.0 mM, 6.0 mL) was mixed with Pro or PAM or HYP solution (1.0 M, 2.0 mL) under stirring. The mixture was stirring at 100 °C for 10.0 min, then, it was centrifuged for 10.0 min at 10,000 rpm to remove any precipitates. The obtained Pro@AuNCs or PAM@AuNCs or HYP@AuNCs were stored at 4 °C for further use.

Detection OFLX by a colourimetric assay

OFLX stock solution (10.0 mM) was prepared and various concentrations were obtained by serial dilution of the stock solution. For testing OFLX, a series of 30.0 μL of standard solutions of OFLX (0.3-1.5 mM) were added into 150.0 μL of POME@AuNCs solution. Then, TMB (36.0 μL, 25.0 mM) and H₂O₂ (90.0 μL, 10.0 M) was mixed with acetate buffer solution (2.70 mL, 12.0 mM, pH 3.0). The final mixture was incubated at 25 °C for 20.0 min before conducting the UV-vis absorption measurements.

Steady-state kinetic study of POME@AuNCs nanozymes

To calculate the steady-state enzymatic kinetic parameters of POME@AuNCs, various concentrations of either TMB or H₂O₂ were prepared in buffer solutions. Double reciprocal Michaelis-Menten curves were plotted and fitted to Lineweaver-Burk equation [1]:

$$1/v = \{(K_m/V_{max}) (1/[S]) + (1/V_{max})\}$$

where V is the initial velocity, K_m is the Michaelis-Menten constant, $[S]$ is the concentration of the substrate, and V_{max} is the maximal reaction velocity.

Selectivity

The interferences (1.0 mM, 30.0 μ L), including glucose, vitamin C, L-Lys, L-Thr, L-His, L-Pro, L-Ser, L-Leu, Ni²⁺, Mg²⁺, K⁺, Ca²⁺, Na⁺ and Zn²⁺, were mixed with POME@AuNCs-TMB-H₂O₂ solution to evaluate the selectivity of the catalytic reaction system.

OFLX metabolic procedure in rat serum

Three male-Sprague-Dawley-rats (about 250 g) were purchased from Beijing Vital River Laboratory Animal Technology Co. Ltd. (Beijing, China). All experiments concerning with rats were complied with the guide for caring and using of laboratory animals from the Association for Assessment and Accreditation of Laboratory Animal Care. The ethical approval of the present study was obtained from the Animal Care and Use Committee.

The controlled blank rat serum samples and five different rat serum samples were collected from the posterior orbital hemorrhage of rats after 14.5 mg/kg OFLX dissolved in physiological saline solution was injected into the tail intravenous of rats (at 0.5 h, 1.5 h, 3.5 h, 5.0 h, 7.0 h). The rat serum samples were pre-treated to eliminate the interferences-proteins. Simply, 0.1 mL of the fresh rat serum samples was diluted by 0.1 mL of water, which was heated in a water-bath to boil for 20.0 min. Consequently, the rat serum samples were centrifuged at 10,000 rpm for 10.0 min and the supernatant was collected and stored at 4 °C for further analysis.

The proposed colorimetric POME@AuNCs-TMB-H₂O₂ system was applied to determine the amount of OFLX in the rat serum samples. 30.0 μ L rat serums, POME@AuNCs solution (150.0 μ L), TMB (36.0 μ L, 25.0 mM), H₂O₂ (90.0 μ L, 10.0 M) and acetate buffer (2.7 mL, 0.2 M, pH 3.0) were mixed. After the mixture was incubated at 25 °C for 10.0 min, the UV-*vis* absorption measurements were conducted [2].

References

- [1] D.L. Wei, X.Y. Zhang, B. Chen, K. Zeng, Using bimetallic Au@Pt nanozymes as a visual tag and as an enzyme mimic in enhanced sensitive lateral-flow immunoassays: Application for the detection of streptomycin, *Anal. Chim. Acta*, 1126 (2020) 106-113.
- [2] L. Shen, Q.F. Zhang, S.M. Tu, W.T. Qin, SIRT3 mediates mitofusin 2 ubiquitination and degradation to suppress ischemia reperfusion-induced acute kidney injury, *Exp. Cell Res.*, 408 (2021) 112861.

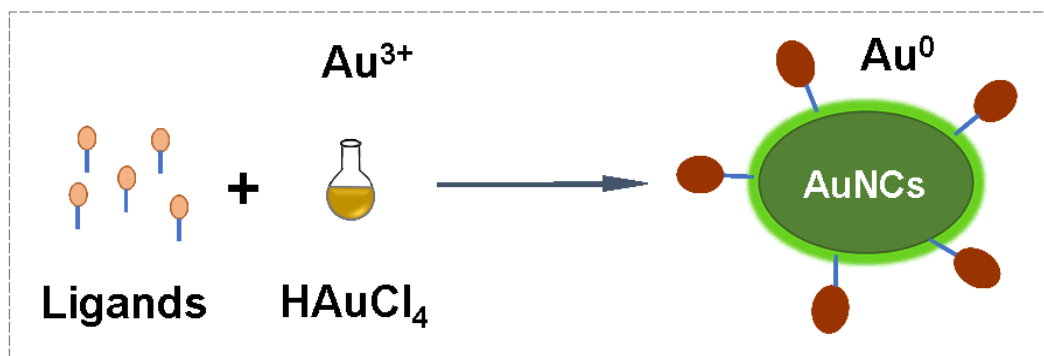


Fig. S1. Preparation of AuNCs protected with Pro, POMe, PAM and HYP as the ligands.

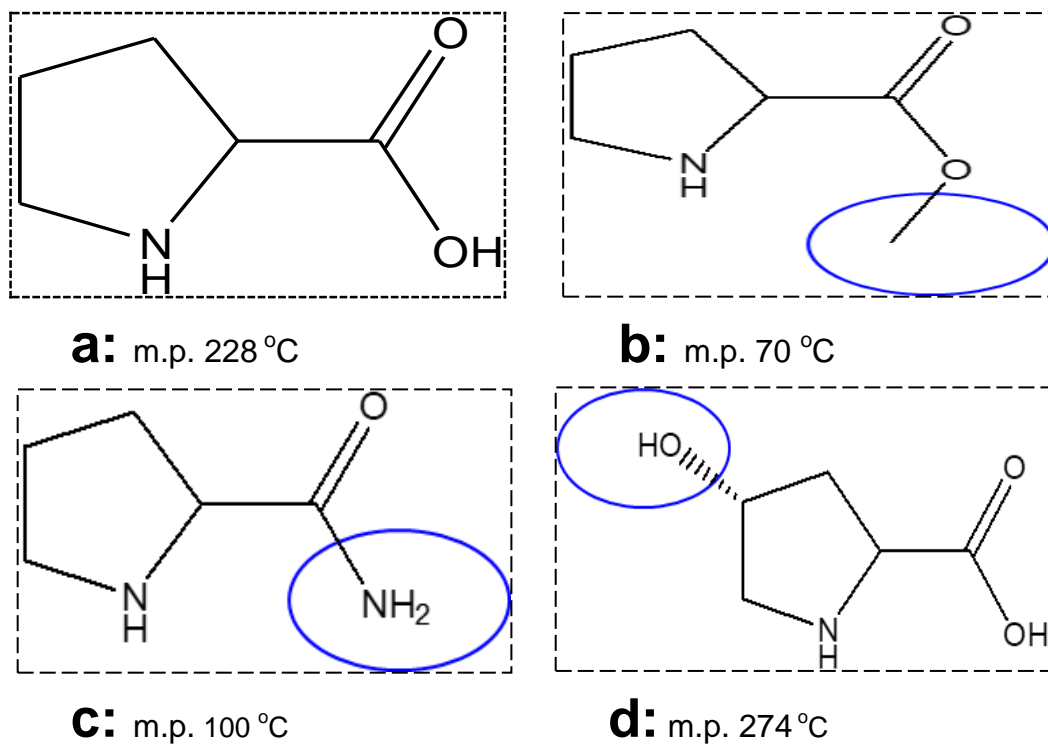


Fig. S2. Structure and melt point (m.p.) of Pro (a); POMe (b); PAM (c) and HYP (d).

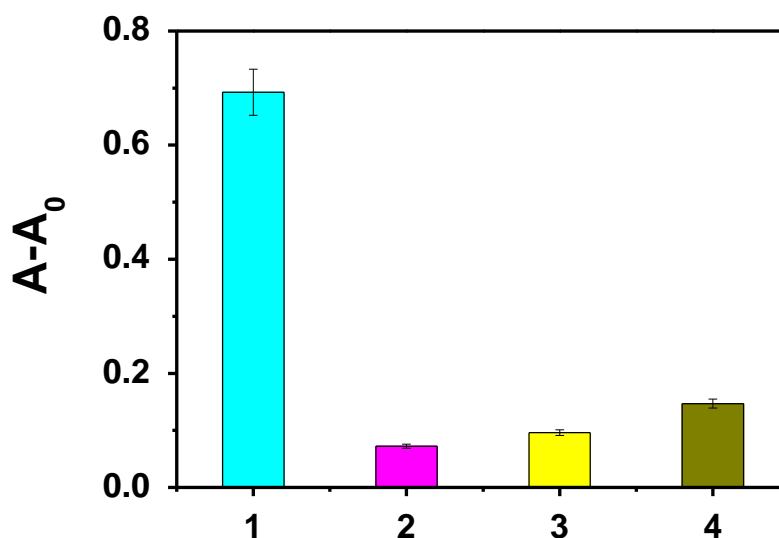


Fig. S3. The relative UV-vis absorbance intensity at 650 nm of the oxidation system in the presence of different nanozymes: 1. POME@AuNCs; 2. Pro@AuNCs; 3. PAM@AuNCs; 4. HYP@AuNCs. A_0 : UV-vis absorbance of AuNCs-TMB- H_2O_2 ; A: UV-vis absorbance of AuNCs-TMB- H_2O_2 -OFLX.

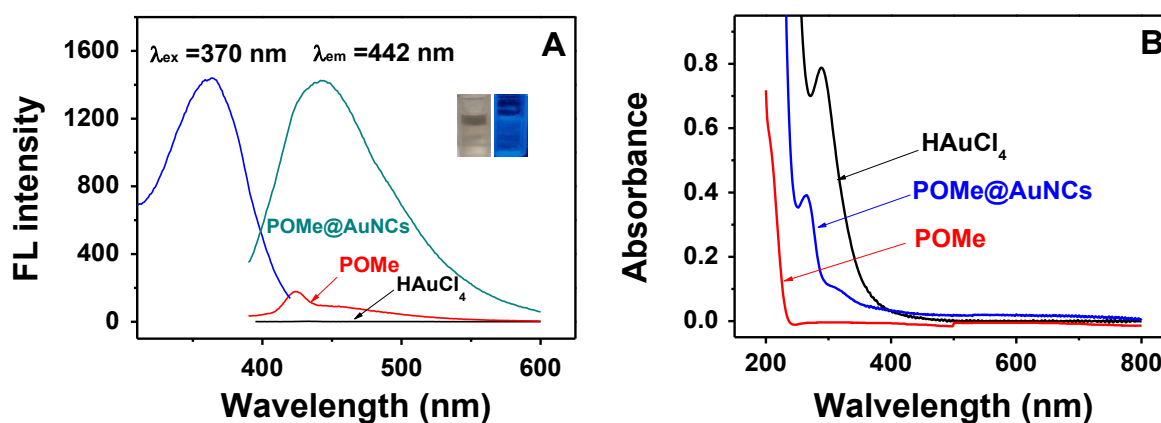


Fig. S4. (A) The excitation and emission spectra of the synthesized POME@AuNCs. Inset: photos of obtained POME@AuNCs solution under white light (left) and excitation source irradiation (right); (B) UV-vis absorption spectra of the aqueous POME@AuNCs, POME, and $HAuCl_4$, respectively.

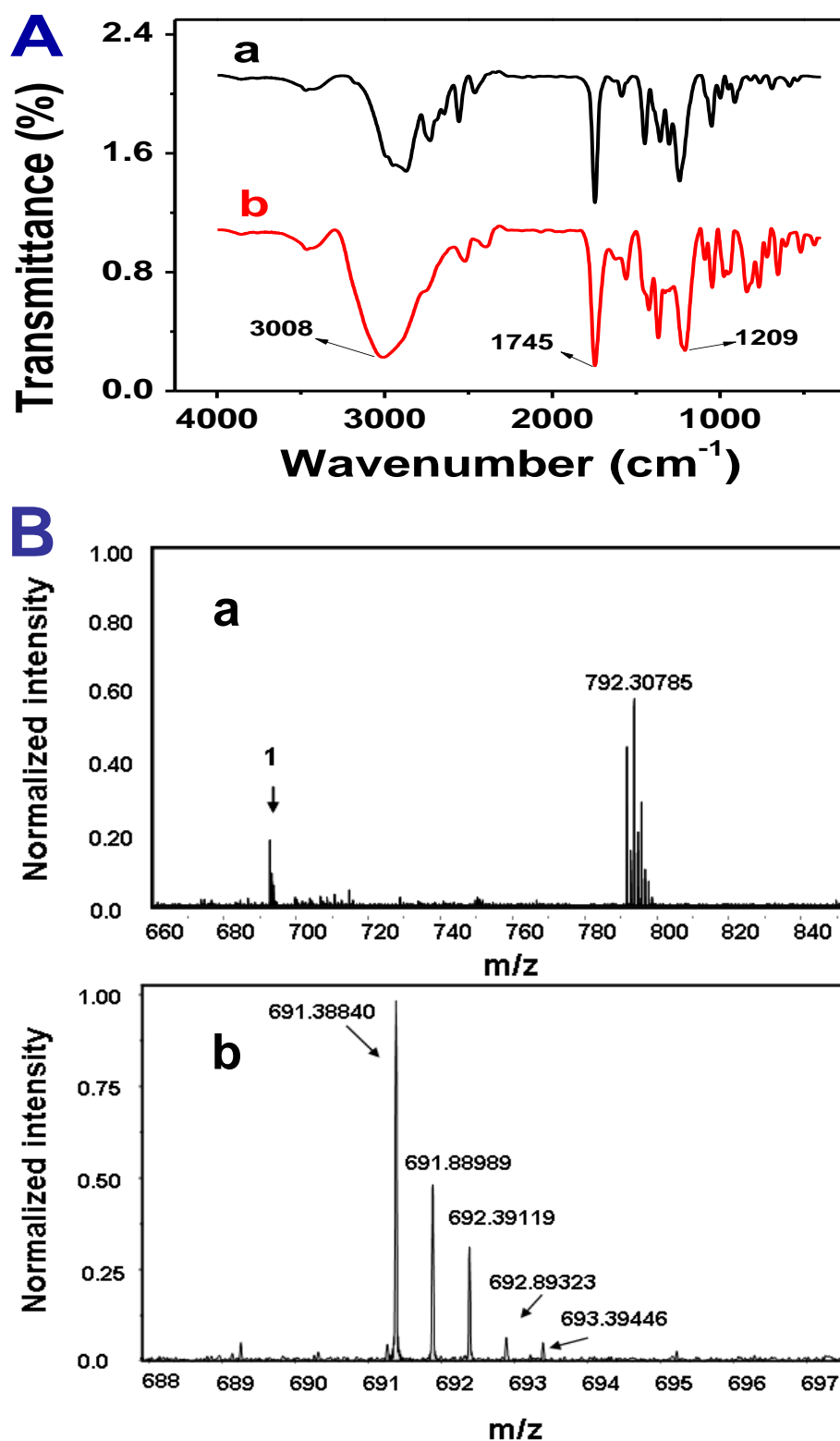


Fig. S5. (A) FT-IR spectra of (a) POME and (b) POME@AuNCs with -NH- groups and -C=O groups. (B) ESI mass spectra of POME@AuNCs (a) $m/z=660-840$. The arrow represents the peaks related to Au_4 clusters encapsulated by POME; (b) Enlarged view of peak 1 originated from $[\text{Au}_4\text{P}_4+2\text{K}]^{2+}$ ($m/z=691.38840$).

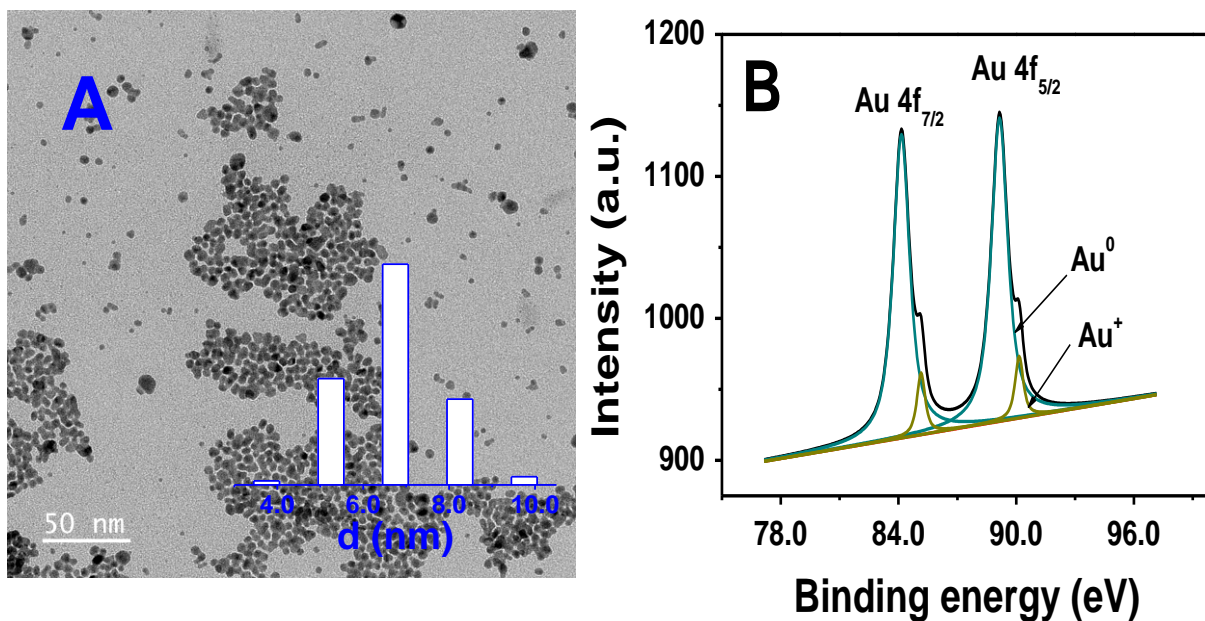


Fig. S6. (A) TEM micrograph of POME@AuNCs, inset: size distribution of POME@AuNCs; (B) XPS spectra of Au 4f orbitals of POME@AuNCs.

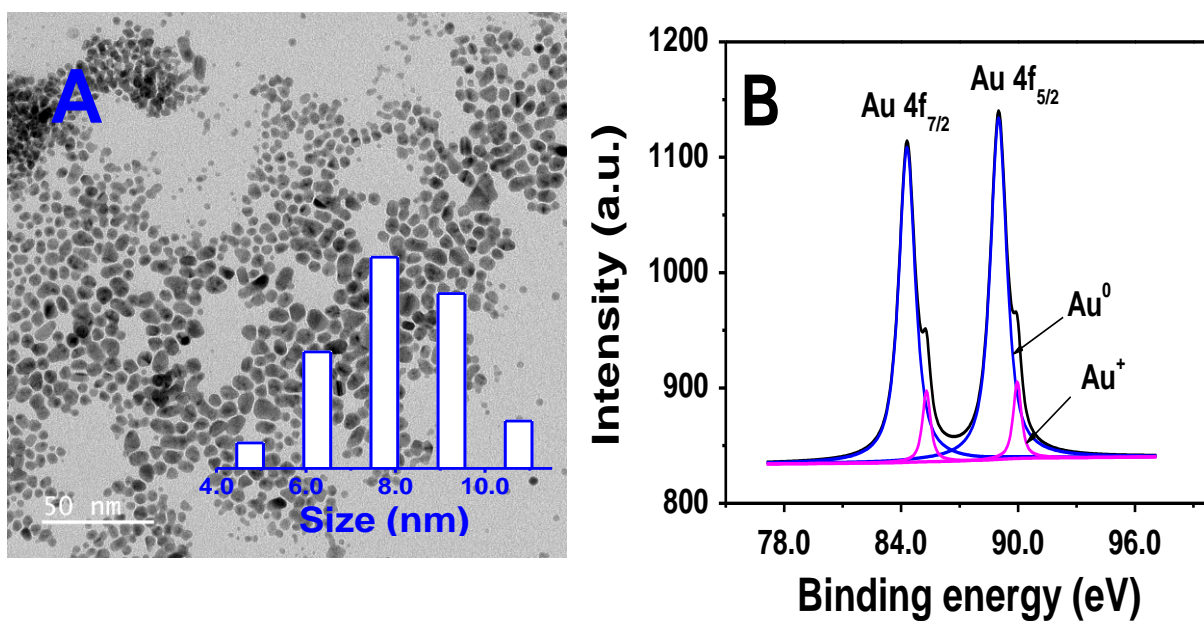


Fig. S7. (A) TEM micrograph of POME@AuNCs-OFLX, inset: size distribution of POME@AuNCs-OFLX; (B) XPS spectra of Au 4f orbitals of POME@AuNCs-OFLX.

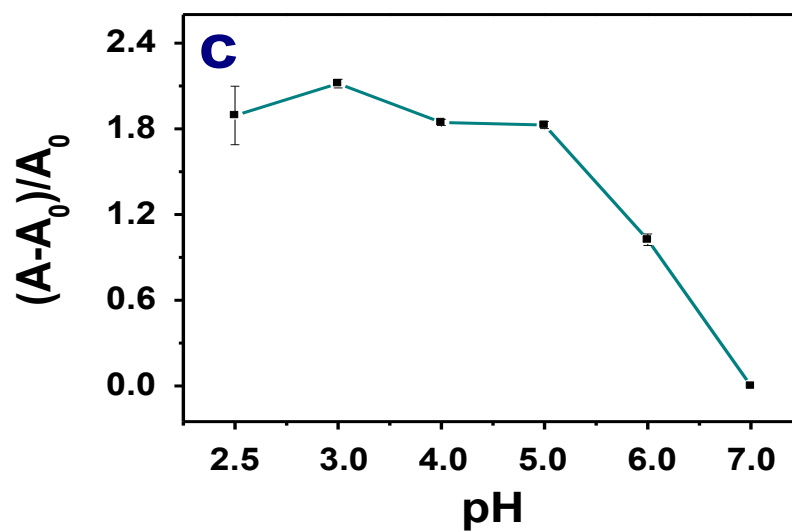
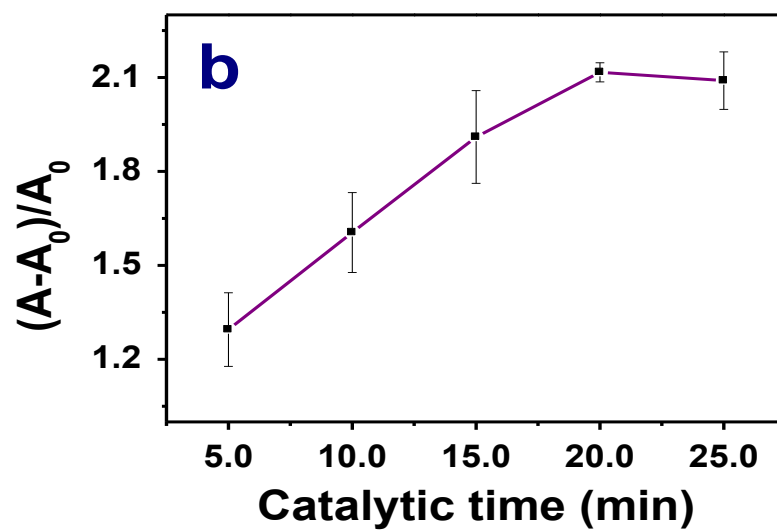
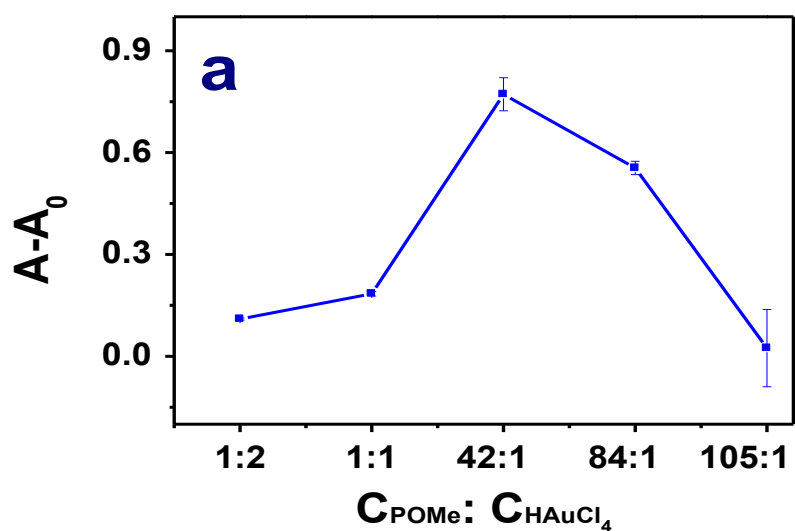


Fig. S8. Effect of concentration ratio (a), catalytic reaction time (b) and pH (c) on the nanozymes catalytic activity in the absence (A_0) and presence of OFLX (A).

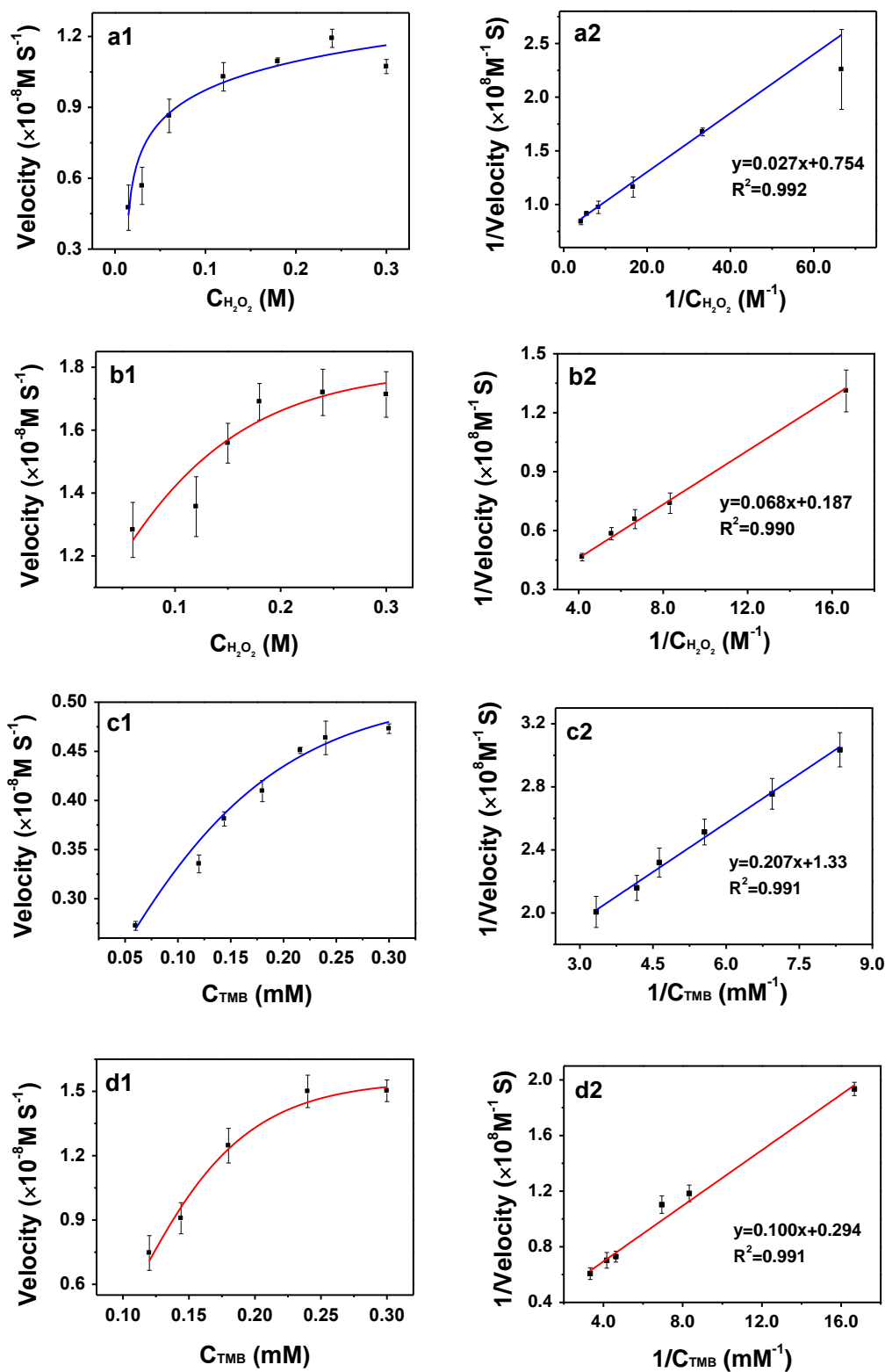


Fig. S9. Steady-state kinetics study of the POME@AuNCs in the absence (a1, a2, c1, c2) and presence (b1, b2, d1, d2) of OFLX. The kinetic data were gained by changing the concentration of one substrate while keeping the concentration constant of the other substrate (0.3 mM TMB or 0.3 M H_2O_2).

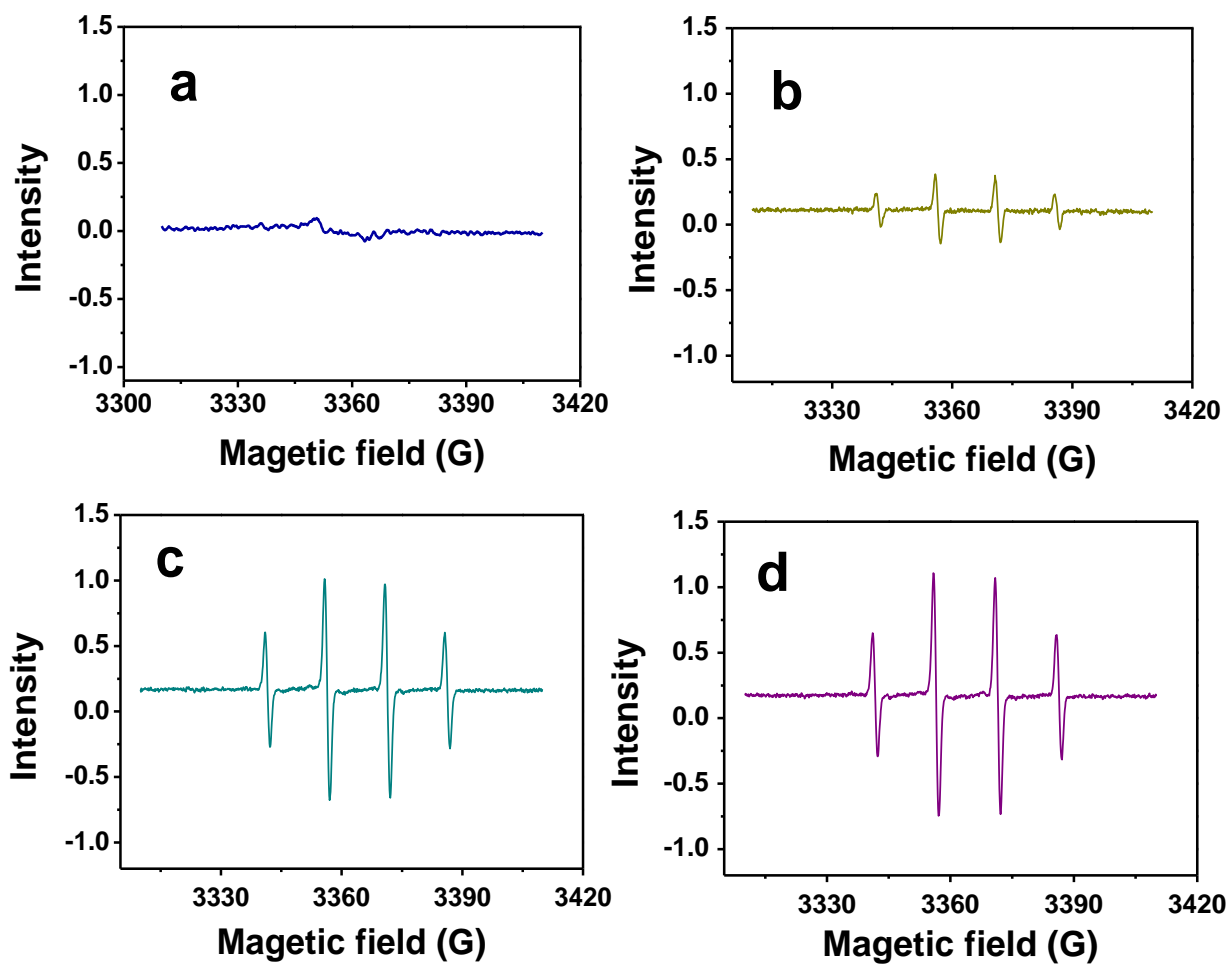


Fig. S10. EPR signals of DMPO (a); DMPO-H₂O₂ (b); DMPO-H₂O₂-POMe@AuNCs (c) and DMPO-H₂O₂-POMe@AuNCs-OFLX (d), respectively. The concentrations of DMPO, H₂O₂ and OFLX were 0.1 M, 0.3 M and 10.0 μ M, respectively.

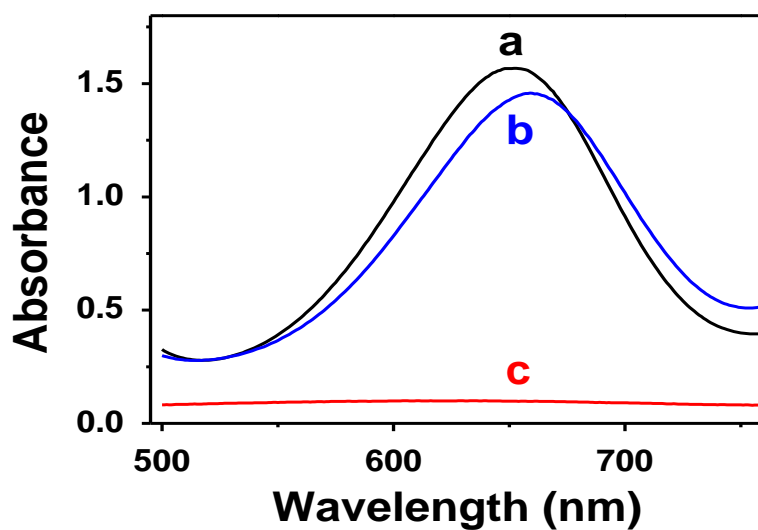


Fig. S11. Effect of radical inhibitors on the POME@AuNCs-TMB-H₂O₂-OFLX absorbance in the absence (a) and presence of t-butyl alcohol (b), benzoquinone (c). (t-butyl alcohol, 0.8 mM; benzoquinone, 0.4 mM).

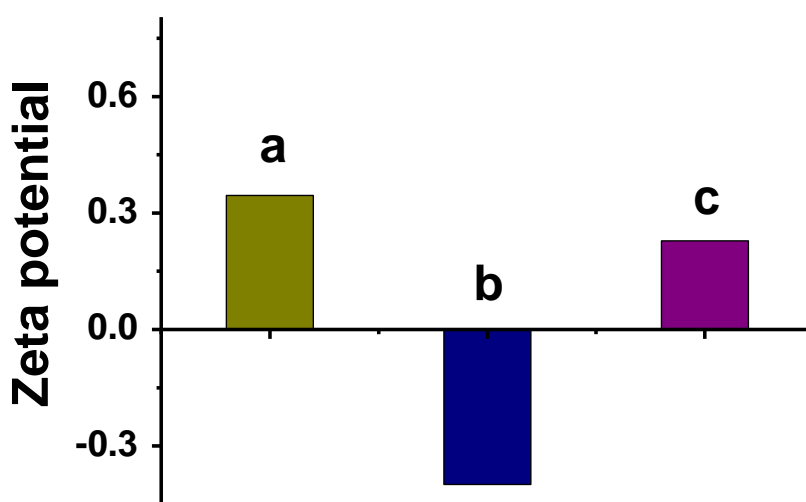


Fig. S12. The apparent zeta potentials of POME@AuNCs (a), OFLX (b) and POME@AuNCs- OFLX (c), at pH 3.0.

Table S1 Comparison with the reported nanozymes in TMB-H₂O₂ system for monitoring of antibiotics

Nanozymes	Synthesis conditions	Test antibiotics	Real samples	References
Fe₃O₄@AuNPs-Apt	25 °C 8.0 h	chloramphenicol	fish	H. Gao, et al. Anal. Meth. 2015, 7, 6528.
Citrate@AuNPs-Apt	25 °C 2.0 h	kanamycin	milk	C. Wang, et al. Biosens. Bioelectron. 2017, 91, 262.
GSH@AuNCs-Apt	90 °C 6.5 h	tetracycline	milk	Z. Zhang, et al. Talanta 2020, 208, 120342
PF127@Pt@AuNPs	25 °C 24.0 h	streptomycin	milk	D. Wei, et al. Anal. Chim. Acta 2020, 1126, 106.
Fe₃O₄@CuNPs	25 °C 2.5 h	tetracycline	milk	L. Wang, et al. Microchim. Acta 2022, 189, 86.
POMe@AuNCs	100 °C 0.17 h	ofloxacin	rat serum	This work

Table S2 Recovery of the assay (n=3)

Rat serums	Added (μM)	Found (μM)	Recovery (%)
1	3.0	3.1	103.3 ± 0.4
	5.0	4.9	98.0 ± 0.36
	10.0	9.6	96.0 ± 0.43
2	3.0	2.8	93.3 ± 0.25
	5.0	5.1	102.0 ± 0.46
	10.0	10.2	102.0 ± 0.47
3	3.0	2.8	93.3 ± 0.49
	5.0	5.2	104.0 ± 0.19
	10.0	10.6	106.0 ± 0.23